TRANSACTIONS ON ELECTRICAL AND ELECTRONIC MATERIALS
Vol. 17, No. 3, pp. 134-138, June 25, 2016

Regular Paper

pISSN: 1229-7607 eISSN: 2092-7592
DOI: http://dx.doi.org/10.4313/TEEM.2016.17.3.134
OAK Central: http://central.oak.go.kr

Efficiency Improvement of Organic Solar Cells Using Two-step Annealing Technique

Bilal Masood†, Arsalan Haider, and Tehsin Nawaz
The Superior College, University Campus, Lahore 54000, Pakistan

Received December 24, 2015; Revised February 19, 2016; Accepted February 22, 2016

The fullerene solar cells are becoming a feasible choice due to the advanced developments in donor materials and improved fabrication techniques of devices. Recently, sufficient optimization and improvements in the processing techniques like incorporation of solvent vapor annealing (SVA) with additives in solvents has become a major cause of prominent improvements in the performance of organic solar cell-based devices . On the other hand, the challenge of reduced open circuit voltage (V_{oc}) remains. This study presents an approach for significant performance improvement of overall device based on organic small molecular solar cells (SMSCs) by following a two step technique that comprises thermal annealing (TA) and SVA (abbreviated as SVA+TA). In case of exclusive use of SVA, reduction in V_{oc} can be eliminated in an effective way. The characteristics of charge carriers can be determined by the measurement of transient photo-voltage (TPV) and transient photo-current (TPC) that determines the scope for improvement in the performance of device by two step annealing. The recovery of reduced V_{oc} is linked with the necessary change in the dynamics of charge that lead to increased overall performance of device. Moreover, SVA and TA complement each other; therefore, two step annealing technique is an appropriate way to simultaneously improve the parameters such as V_{oc}, fill factor (FF), short circuit current density (J_{sc}) and PCE of small molecular solar cells.

Keywords: SMSCSs, TA, SVA, FF, PCE

1. INTRODUCTION

In the last decade, SMSCSs have gained remarkable attention from industry, academia, research and development around the globe due to its cost effective processing such as roll to roll manufacturing and ink jet printer etc. Due to the cost effectiveness of SMSCSs, it has become an indispensible candidate of renewable energy sources that can be fabricated on a large scale. It has several features that include the high potential degree of crystallization, properly defined structure and ease of purification. [1-4]. The rapid growth of emerging small semiconducting molecules and improved device fabrication techniques, has led to the overall performance of SMSCs approaching their polymer counterparts, known as polymer solar cells [5]. It comprises the combination of π conjugated, p-type polymer, and fullerene n-type acceptor [6,7].

The efficiencies of SMSCSs still require improvement to achieve the standard of their polymer counterparts. The goal of improved SMSCSs device performance can be achieved by research and development focused on the latest device structures, material systems and optimized processing techniques. TA, SVA and solvent additives are amongst the most promising optimized processing techniques of various existing methods [8-11]. These techniques are successfully incorporated and enhance the performance of SMSCSs device by utilizing various donor systems, but with the tradeoff in reduction of V_{oc} [11-14]. The previous literature deals with the nano-scale and electrical steady-state characterization of film morphology. However, the effect of these techniques on charge dynamics present in the operated devices is rarely evaluated.

This paper presents the charge dynamics in very effective SMSCSs through measurements of TPV and TPC that directly

† Author to whom all correspondence should be addressed:
E-mail: bilalmasood84@yahoo.com

Copyright ©2016 KIEEME. All rights reserved.
This is an open-access article distributed under the terms of the Creative Commons Attribution Non-Commercial License (http://creativecommons.org/licenses/by-nc/3.0) which permits unrestricted noncommercial use, distribution, and reproduction in any medium, provided the original work is properly cited.

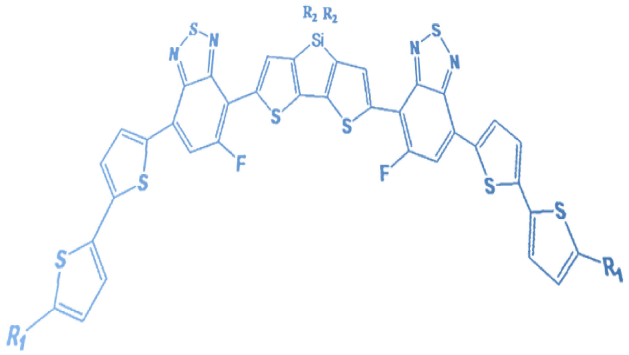

Fig. 1. The chemical structures of p-DTS(FBTTh$_2$)$_2$.

corresponds to the charge recombination [15-18]. The fabrication of SMSCSs were performed from the blend of, 7,7□ -(4,4-bis (2-ethylhexyl) -4H-silolo [3,2-b:4,5-b□] dithiophene-2,6-diyl) bis (6-fluoro-4- (5□-hexyl- [2,2□-bithiophen]-5-yl) benzo [c] [1,2,5] thiadiazole) (p-DTS(FBTTh$_2$)$_2$) (chemical structure shown in Fig. 1) [7]; and [6,6]-phenyl C71 butyric acid methyl-ester (PC$_{71}$BM), with sufficiently improved device performance by vapor processing of dichloromethane (DCM) and further improvement capacity by consequential TA.

2. DETAILS OF EXPERIMENTAL SETUP

The structure of device used in this research work is ITO/PEDOT: PSS/p-DTS (FBTTh$_2$)$_2$: PC$_{71}$ BM/PFN/Al, where ITO denotes the Indium Tin Oxide, PFN denotes the poly [(9, 9-bis(3□ - (N,N-dimethylamino) propyl) - 2, 7 - fluorene) - alt -2,7-(9,9-dioctylfluorene)] (PFN) and PEDOT: PSS represents the poly (3,4-ethylenedioxythiophene): poly (styrenesulfonate) (purchased from Clevios P PVP AI 4083, H.C starck Inc.) [19]. The cleaning of ITO coated glass substrates was performed with the help of detergent, sequential sonication in acetone, alcohol (isopropyl) and deionized water, followed by baking at 85℃ for the duration of 12 hours in vacuum oven. A PEDOT layer of PSS with a thickness of 40 nm was spin coated on the already cleaned plasma treated substrates of ITO-glass and dried at the temperature of 150℃ for the duration of 20 minutes. PC17BM and p-DTS (FBTTh$_2$)$_2$ were dissolved together into a blend of chlorobenzene at a ratio of 1:1 with 38 mg/mL overall concentration, with stirring over night. The 90 nm thick active layer of films were spin coated with the solution at 95℃. Furthermore, the resultant active layer of films was transferred into a wide-mouthed bottle and treated for 30 seconds from a saturated vapor of DCM, meanwhile treatment of films was performed at 100℃ for 1 min duration (compulsory) from TA. Subsequently, a cathode interlayer of PFN with 5 nm thickness was spin coated over the active layer. Finally, the deposition of Al electrode of 80 nm was performed with the help of thermal evaporation from a shadow mask at 2×10^{-4} Pa base pressure in a vacuum chamber. However, the encapsulation of finished devices using UV epoxy was completed before testing. The measurement apparatus, Keithley 2400 source at illumination of 1.5G (AM) was used with the help of solar simulator, which has Oriel model 91192 for measurement purpose. The calibrations were carried out by reference cell of silicon (Hamamatsu S1133). The steady state measurements of light intensity dependent parameters J_{sc} and V_{oc} were performed; whereas, utilizing neutral density filters with a range of optical density 0.2 - 2, different light intensity was observed. The photodetector responsibility measurement system by Enlitech Inc. was utilized in order to measure external quantum efficiency (EQE).

Table 1. Parameters for the performance of devices with different treatment of annealing (under 100 mW/cm^2, AM 1.5G Illumination).

Treatment	V_{oc} (V)	J_{sc} (mA/cm^2)	FF (%)	PCE (%)
None	0.79	8.71	34.5	2.33%
SVA	0.77	14.85	65.8	7.51%
SVA+TA	0.81	15.3	67.6	8.25%

The testing of carriers' mobility was carried out in dark by using Mott-Gurney equation as,

$$J = 9/8\ \varepsilon_0\ \varepsilon_r\ \mu v^2/L^3$$

where, J denotes the current density, ε_r represents relative permittivity of active layer, ε_0 is permittivity of free space, L is thickness of film and V represents effective voltage that is obtained by $V = V_{app} - V_{bi}$, where V_{app} and V_{bi} denotes the applied and building voltages, respectively. The structure of devices in case of hole only device is ITO/PEDOT: PSS/p-DTS (FBTTh$_2$)$_2$:PC$_{71}$BM/MoO$_3$/Al and in case of electron only device is ITO/ZnO/PFN/p-DTS (FBTTh$_2$)$_2$: PC$_{71}$BM/PFN/Al.

A well-known experimental procedure is used for TPC and TPV [12,14]. The laser excitation was with pulse width 8 ns, at 532 nm and 20 Hz frequency. The signal was obtained for measurement of TPV from Tektronix DPO4014 oscilloscope that has input impedance of 1 MΩ under the condition of open circuit. In order to adjust the V_{oc} of the devices, 100 W tungsten lamp of bromine was tuned for its illumination intensity by incorporating neutral density filters, generating 1 and 100 mW/cm^2 steady state illumination intensity. The TPV amplitude is kept 5 % less than V_{oc} by attenuating the pulsed laser power with a set of neutral density filter. The measurement of TPC was carried out using oscilloscope of Tektronix DPO4014 by obtaining TPV across a load resistance of 50 Ω. The data was averaged from 32 measurements. The deduction for the concentration of charge carriers from TPC and TPV was as previously recommended [15,20].

3. RESULTS AND DISCUSSION

The steady state J versus V plots from various types of treatments are depicted in Fig. 2; whereas, the parameters to obtain the performance of device are tabulated in Table 1. In case of without annealing of device, 2.33% moderate PCE was achieved along with J_{sc} and V_{oc} of 8.71 mA cm^{-2} 0.79 V, respectively, with fill factor of 34.5%. A drastic improvement in the performance of device was observed after proper SVA that resulted in 7.51% PCE. The main reason of this improvement was prominent improvements in J_{sc} and FF with 14.85 mA cm^2 and 65.8%, respectively; whereas, a slight decrease in V_{oc} due to more current leakage as J versus V plots are shown in Fig. 3. Notably, the overall device performance can be improved by further treatment of TA after SVA treatment. After achieving the overall device performance, a simultaneous improvement was observed in the parameters of device resulting in an increase in PCE to 8.25%.

A similar efficiency improvement is observed in J_{sc}, the EQE plot of each device is shown in Fig. 4. A clear improvement in EQE is observed within the range of 300 to 725 nm. Moreover, a slight improvement in EQE is also observed in case of TA treatment right after SVA (SVA+TA). Previous literature [12,13] does not present evaluation of the treatment effect over the dynamics of charge.

In order to examine the origin of enhanced performance of

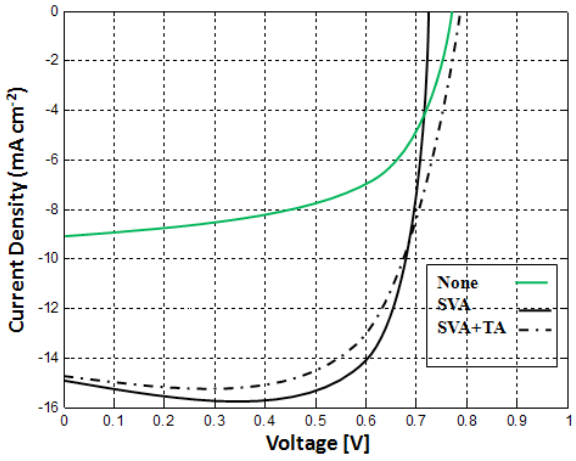

Fig. 2. Characteristics of Voltage versus Current Density of SMSC with various annealing treatments under AM 1.5 G, 100 mW/cm^2 in irradiation.

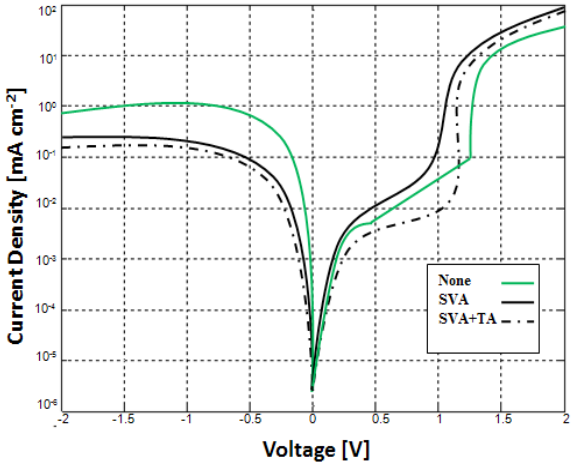

Fig. 3. Characteristics of Voltage versus Current Density of SMSC with various annealing treatments under AM 1.5 G, 100 mW/cm^2 in dark.

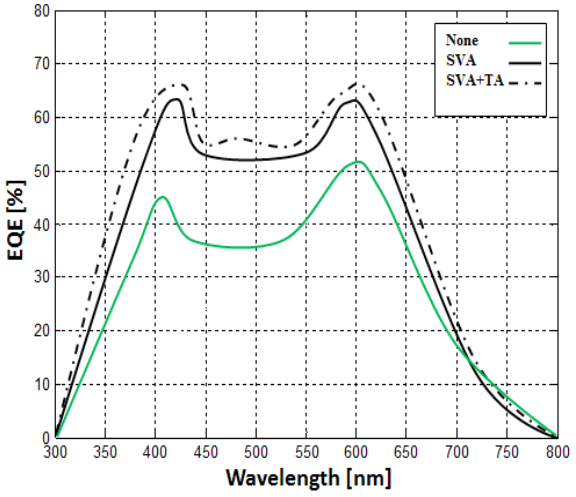

Fig. 4. EQE spectra of solar cells under various annealing treatments.

device on SVA and TA, we investigated the mobility of charge carriers in the devices, as shown in Figs. 5 and 6. The plots elu-

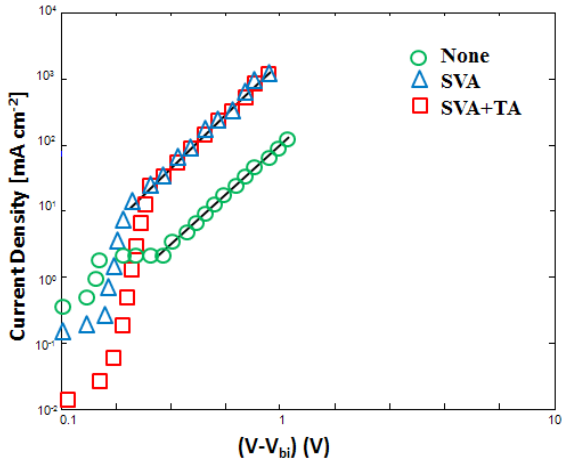

Fig. 5. Characteristics of Voltage versus Current Density of single charge carrier with various annealing treatment for devices with hole only. Solid line is best fitting plot.

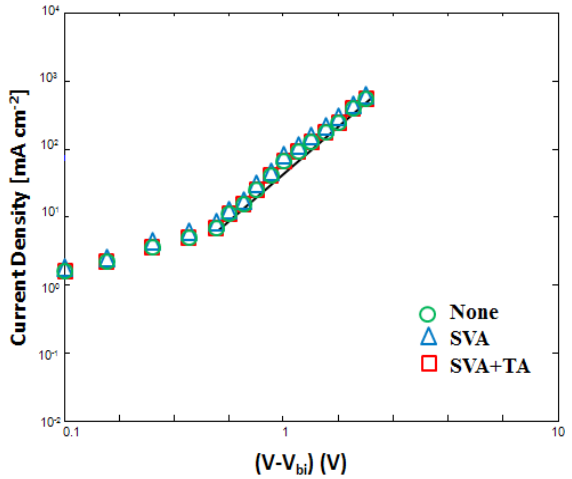

Fig. 6. Characteristics of Voltage versus Current Density of single charge carrier with various annealing treatment for devices with electron only. Solid line is best fitting plot.

cidate the J_{sc} vs. V characteristics for the devices of single charge carriers by utilizing various treatments, where high bias of J_{sc} vs. V plots can be explained by Mott-Gurney equation. The obtained mobility of electron and hole were found as 3.4×10^{-4} cm^2/Vs and 8.1×10^{-6} cm^2/Vs, respectively in untreated film. The main limiting factor clearly is smaller mobility of hole, which is a root cause of poor performance in untreated devices that reduces J_{sc} and FF [21].

However, mobility of holes is increased to 9.4×10^{-5} cm^2/Vs indicative of enhancement in magnitude approximately. On the other hand, mobility of electron of approximately 3.6×10^{-4} cm^2/Vs does not change. In summary, the overall performance of device was dramatically improved whereby a slight decrease in V_{oc} of 0.77 V was observed, as previously reported [11,22-24]. The cause of decrease in V_{oc} is linked with the decrease in Quasi-Fermi levels for the transport of hole and electron [25,26]. The mobility of hole increased further to 1.1×10^{-4} cm^2/Vs when applying TA after SVA; whereas, mobility of electron increased moderately to 3.9×10^{-4} cm^2/Vs resulting in simultaneous improvement of all device parameters. By following the TA treatment, reduction in V_{oc} can be controlled.

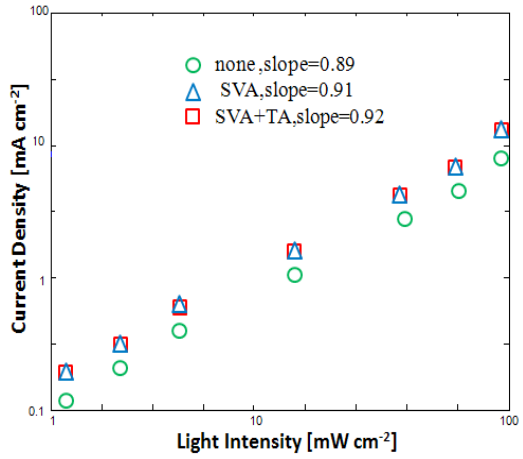

Fig. 7. J_{sc} versus light intensity experimental results for various annealing treatment devices.

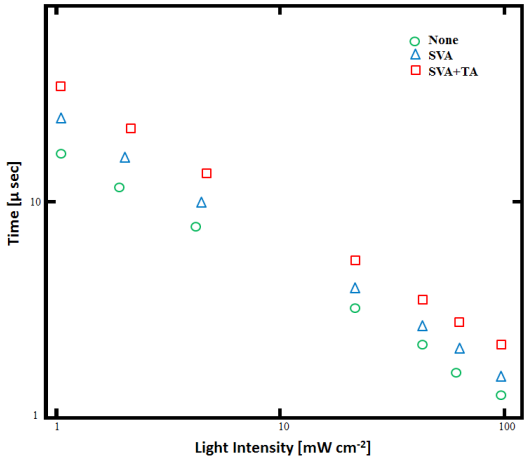

Fig. 10. Lifetimes of carriers with respect to intensity of light with various annealing treatment of devices.

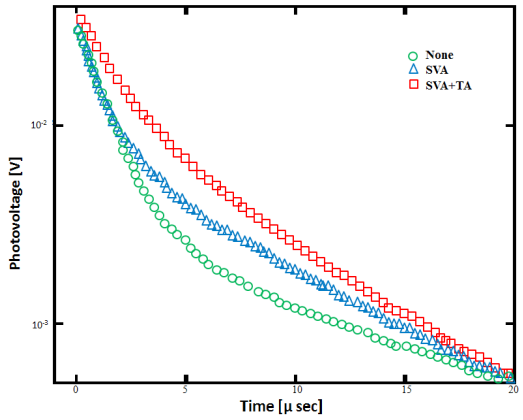

Fig. 8. Measurement of TPV with various annealing treatment devices with 100 mW/cm^2 light intensity bias.

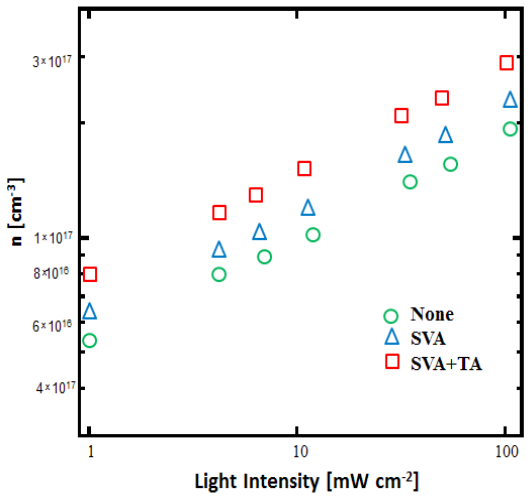

Fig. 11. Concentrations of carriers with respect to intensity of light with various annealing treatment of devices.

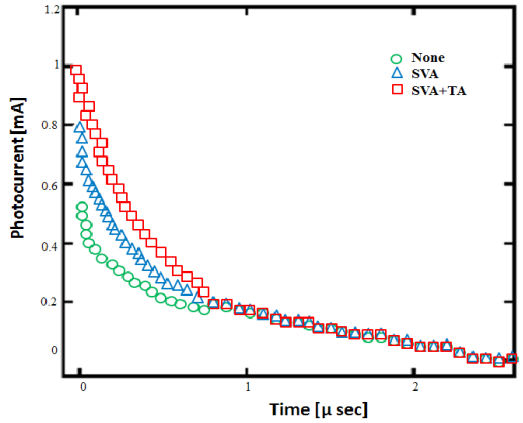

Fig. 9. Measurement of TPC with various annealing treatment devices without bias.

Measurements of J_{sc} dependent on light intensity were carried out at a range of the illumination intensity between 1-100 mW/cm^2, by following the relation; $J_{sc} \alpha I^{\alpha}$, where α denotes the exponential entity, where α is representing the exponential factor. The values of α that can be used for most appropriate fitting in case of pristine device, the device treated by SVA treatment and the two-step annealing process (SVA+TA) are 0.89, 0.91 and 0.92, respectively, which reflects the increasing suppression of bimolecular recombination loss in the said devices as a result of change in charge carrier dynamics [27]. Mutual dependency of current density and intensity of light is evaluated as shown in Fig. 7 [13]. We further used the measurements of TPC and TPV so that dynamics of carrier recombination in devices can be evaluated. After utilizing the various treatments on devices, the measurement results of TPV are illustrated in Fig. 8. The results are obtained using a light bias with 100 mW/cm^2 intensity, which is the same as real working condition. TPV can be explained by following $\delta V = Vp\ e^{(-t/\tau)}$ [12]. Where τ represents the lifetime of charge carrier with value 2.1 μs for SVA treated device and 1.6 μs (untreated device), thereby 2.8 μs lifetime was obtained in case of SVA+TA. The lifetime dependence of carriers vs. illumination light intensity (1-100 mW/cm^2) for various devices by taking double log is shown in Fig. 9; the result show the same trend as depicted in Fig. 8.Thus, product of mobility lifetime was enhanced significantly. In conclusion, the efficiency of charge collection and property of charge transport, after the treatment is improved resulting in less loss of bimolecular recombination and improved FF and J_{sc}.

As illustrated in Fig. 10, the results of TPC measurement prove

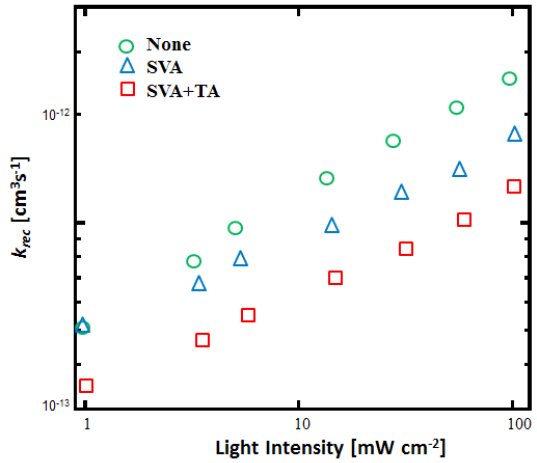

Fig. 12. Calculated K_{rec} versus intensity of light with various annealing treatment of devices.

that efficiency of charge extraction in the untreated device is lowest. The carrier concentration dependency vs. intensity of light in various devices is depicted in Fig. 11 based on available literature [13,14,17]. It is evident from the results shown in Fig. 11 that SVA + TA treated device produces more photo generated carriers for all illumination range followed in research.

The bimolecular rate factor for recombination, denoted by K_{rec} can be calculated from Figs. 9 and 11, where $K_{rec} = 1/2\tau n$ [15]; the results are shown in Fig. 12. The K_{rec} is maximum in the pristine device by utilizing the minimum concentration of carrier (n), followed by SVA device, however, processing the device with two step annealing resulted in minimum K_{rec}. The V_{oc} dependence of organic solar cell is not only on electronic levels of acceptor and donor, but is also dependent on the magnitude of K_{rec}. The V_{oc} increased by 80 mV with a decrease of one order of magnitude in K_{rec}. Therefore, varying the charge dynamics results in the reduction of K_{rec} by (half in comparison to pristine device), the 40 mV enhancements corresponds to SVA+TA, whereas enhancement of 10-20 mV in the device with treatment of SVA.

4. CONCLUSIONS

This study presents the approach to significantly improve the overall performance of organic SMSCSs device by utilizing a two step technique comprising SVA and TA. This technique will improve the conversion efficiency of power by 8.25%; whereas, solely SVA also improves the efficiency greatly, but with a tradeoff of reduction in V_{oc}. The use of SVA exclusively can increase the magnitude in the mobility of hole that is beneficial for collection and transport of charge; on the other hand, the depleted steady carrier density causes the decrease in V_{oc}. The reduction of V_{oc} can be effectively eliminated by the consequent treatment of TA that changes the dynamics of charge, thus providing a good overall device performance and V_{oc} improvement. In conclusion, the two step annealing processes provide an appropriate path to simultaneous enhancement in J_{sc}, V_{oc}, PCE and FF SMSCSs.

REFERENCES

[1] J. E. Coughlin, Z. B. Henson, G. C. Welch, and G. C. Bazan, *Acc. Chem. Res.*, **47**, 257 (2013). [DOI: http://dx.doi.org/10.1021/ar400136b]

[2] Q. Zhang, B. Kan, T. P. Russell, and Y. Chen, *Nature Photon.*, **9**, 35 (2015). [DOI: http://dx.doi.org/10.1038/nphoton.2014.269]

[3] Y. Sun, G. C. Welch, W. L. Leong, C. J. Takacs, and G. C. Bazan, *Nature Mater.*, **11**, 44 (2012). [DOI: http://dx.doi.org/10.1038/nmat3160]

[4] Y. Liu, C. C. Chen, Z. Hong, J. GAO, and Y. Yang, *Sci. Rep.*, **3**, 3356 (2013).

[5] C. Zhong, S. Su, M. Xu, H. Wu, and Y. Cao, *Nature Photon.*, **6**, 591 (2012).

[6] B. Kan, Q. Zhang, M. Li, X. Wan, W. Ni, G. Long, Y. Wang, X. Yang, H. Feng, and Y. Chen, *J. Amer.Chem. Soc.*, **136**, 15529 (2014). [DOI: http://dx.doi.org/10.1021/ja509703k]

[7] V. Gupta, S. Chand, G. C. Bazan, and A. J. Heeger, *Sci. Rep.*, **3**, 1965 (2013).

[8] G. Li, V. Shrotriya, J. Huang, Y. Yao, T. Moriarty, K. Emery, and Y. Yang, Nature Mater., 4, 864 (2005). [DOI: http://dx.doi.org/10.1038/nmat1500]

[9] L. Zheng, J. Liu, Y. Ding, and Y. Han, J. Phys. Chem. B, 115, 8071 (2011). [DOI: http://dx.doi.org/10.1021/jp2030279]

[10] Z. Huang, E. C. Fregoso, S. Dimitrov, and J. R. Durrant, *J. Mater. Chem. A*, **2**, 19282 (2014). [DOI: http://dx.doi.org/10.1039/C4TA03589E]

[11] B. Walker, A. B. Tamayo, X. D. Dang, and T. Q. Nguyen, *Adv. Funct. Mater.*, **1**, 3063 (2009). [DOI: http://dx.doi.org/10.1002/adfm.200900832]

[12] K. Sun, Z. Xiao, E. Hanssen, and D. J. Jones, *J. Mater. Chem. A*, **2**, 9048 (2014). [DOI: http://dx.doi.org/10.1039/c4ta01125b]

[13] J. Liu, L. Chen, B. Gao, X. Cao, Y. Han, Z. Xiea, and L. Wanga, *J. Mater. Chem. A*, **1**, 6216 (2013). [DOI: http://dx.doi.org/10.1039/c3ta10629b]

[14] J. Peet, J. Y. Kim, N. E. Coates, W. L. Ma, D. Moses, A. J. Heeger, and G. C. Bazan, *Nature Mater.*, **6**, 497 (2007). [DOI: http://dx.doi.org/10.1038/nmat1928]

[15] C. G. Shuttle, B. O'Regan, A. M. Ballantyne, and J. R. Durrant, *Appl. Phys. Lett.*, **92**, 183501 (2008). [DOI: http://dx.doi.org/10.1063/1.3006316]

[16] Z. Li, F. Gao, N. C. Greenham, and C. R. McNeill, *Adv. Funct. Mater.*, **21**, 1419 (2011). [DOI: http://dx.doi.org/10.1002/adfm.201002154]

[17] C. G. Shuttle, A. Maurano, R. Hamilton, B. O'Regan, J. C. de Mello, and J. R. Durrant, *Appl. Phys. Lett.*, **93**, 183501 (2008). [DOI: http://dx.doi.org/10.1063/1.3006316]

[18] P. P. Boix, J. Ajuria, R. Pacios, and G. G. Belmonte, *Appl. Phys. Lett.*, **109**, 074514 (2011).

[19] A. Semlyen, *IEEE Trans. Power App. Syst.*, **PAS-100**, 848 (1981). [DOI: http://dx.doi.org/10.1109/TPAS.1981.316943]

[20] A. Semlyen and A. Roth, *IEEE Trans. Power App. Syst.*, **96**, 667 (1977). [DOI: http://dx.doi.org/10.1109/T-PAS.1977.32378]

[21] T. Kirchartz, B. E. Pieters, K. Taretto, and U. Rau, *Phys. Rev. B.*, **80**, 035334 (2009). [DOI: http://dx.doi.org/10.1103/PhysRevB.80.035334]

[22] G. Wei, S. Wang, K. Sun, M. E. Thompson, and S. R. Forrest, *Adv. Energy. Mater.*, **1**, 184 (2011). [DOI: http://dx.doi.org/10.1002/aenm.201100045]

[23] H. C. Liao, C. S. Tsao, Y. C. Huang, M.H. Jao, K. Y. Tien, C. M. Chuang, C. Y. Chen, C. J. Su, U. S. Jeng, Y. F. Chend, and W. F. Su, *RSC Adv.*, **4**, 6246 (2014). [DOI: http://dx.doi.org/10.1039/c3ra45619f]

[24] C. D. Wessendorf, G. L. Schulz, A. Mishra, and P. Bauerle, *Adv. Energy Mater.*, **4**, 1400266 (2014). [DOI: http://dx.doi.org/10.1002/aenm.201400266]

[25] W. Chen, D. C. Qi, Y. L. Huang, H. Huang, Y. Z. Wang, S. Chen, X. Y. Gao, and A.T.S. Wee, *J. Phys. Chem. C*, **113**, 12832 (2009). [DOI: http://dx.doi.org/10.1021/jp903139q]